Heliyon 10 (2024) e37223

Contents lists available at ScienceDirect

Heliyon

journal homepage: www.cell.com/heliyon

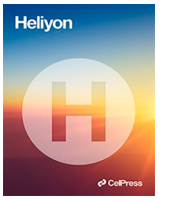

Research article

High doses of radiation cause cochlear immunological stress and sensorineural hearing loss

Mengwen Shi [a,1], Ye Wang [b,1], Huiwen Yang [a,1], Chengcai Lai [c], Jintao Yu [a,**], Yu Sun [a,*]

[a] Department of Otorhinolaryngology, Union Hospital, Tongji Medical College, Huazhong University of Science and Technology, Wuhan, 430022, China
[b] Cancer Center, Union Hospital, Tongji Medical College, Huazhong University of Science and Technology, Wuhan, 430022, Hubei, China
[c] Department of Pharmaceutical Sciences, Beijing Institute of Radiation Medicine, Beijing, 100850, China

ARTICLE INFO

Keywords:
Radiation
Sensorineural hearing loss
Macrophage
Cochlear inflammation

ABSTRACT

Radiotherapy is a crucial treatment for head and neck malignancies, but it can sometimes cause sensorineural hearing loss (SNHL). Changes in the immune microenvironment and sensory neuroepithelium of the inner ear after radiation exposure remain poorly understood. This study investigated cochlear morphology and macrophages in the inner ear after high-dose irradiation. The heads of heterozygous 8-week-old Cx3cr1$^{GFP/+}$ male mice were irradiated with 30Gy of X-rays and biological samples were collected on days 1, 7, and 10 after irradiation. Auditory brainstem responses were used to assess auditory function in the mice. Changes in basilar membrane hair cells, spiral ganglion neurons (SGN), and inner ear macrophages were observed using hematoxylin-eosin (HE) staining and immunofluorescence staining. The expression of inflammatory mediators in the inner ear was detected by quantitative real-time reverse transcription-polymerase chain reaction (RT-qPCR) in cochlear tissue. The results showed no significant hair cell loss after a single high dose of radiation. However, the mice developed pantonal hearing loss on day 10 when HE staining revealed SGN atrophy and immunofluorescence showed decreased neurofilament expression. The number of macrophages in the inner ear reduced over time. RT-qPCR showed that cochlear inflammatory factors and chemokines were briefly upregulated on day 1st after irradiation and then decreased over time. In conclusion, high-dose irradiation causes acute SNHL that is not associated with hair cell loss and may be related to SGN changes. Radiation-induced SNHL is associated with a reduction in cochlear macrophages and changes in the immune microenvironment, but the relationship between the two remains to be investigated.

1. Introduction

Radiotherapy is an important treatment for head and neck tumors. However, it is often difficult to avoid exposure of the temporal bone and its accessory structures to ionizing radiation during the treatment, resulting in damage to the auditory pathways [1,2]

* Corresponding author.
** Corresponding author.
E-mail addresses: jintaoyu@hust.edu.cn (J. Yu), sunyu@hust.edu.cn (Y. Sun).
[1] These authors contribute equally to this work.

https://doi.org/10.1016/j.heliyon.2024.e37223
Received 16 April 2024; Received in revised form 2 August 2024; Accepted 29 August 2024
Available online 31 August 2024

including conductive hearing loss (such as otitis media, ossicular chain necrosis, etc.) and sensorineural hearing loss, which manifests as delayed, progressive and irreversible hearing loss, often with high-frequency hearing loss as the first [3]. In an open-label, randomized phase 2 trial for oropharyngeal squamous cell carcinoma, radiation-induced sensorineural hearing loss (RISNHL) occurred in 38 % of patients after radiotherapy [4]. Research in children with head-and-neck tumors confirms that the onset of high-frequency hearing loss is accelerated by platinum-based chemotherapy when the average cochlear radiation dose is > 20 Gy. Patients develop a rapid onset of low-frequency hearing loss after early high-dose radiation (>30 Gy) regardless of platinum exposure, and this RISNHL continues to increase in incidence over time [5]. Although the timing and degree of ototoxicity after radiotherapy varies clinically, and the correlation relationship between ototoxicity and ionizing radiation dose remains unclear, it is of particular interest to study the pathogenesis of RISNHL.

It is widely accepted that changes in inner ear morphology and auditory pathways after ionizing radiation are widely recognized to be related to tissue absorption dose and exposure time. Currently, the oxidative stress-apoptosis theory [3,6,7] is the prevailing view to explain the dysfunction and death of cochlear hair cells in RISNHL. Ionizing radiation directly causes DNA damage and produces excessive reactive oxygen species (ROS) in tissues [8,9]. Radiation-induced tissue cell death is confirmed by the generation of ROS and subsequent caspase activation, inflammation, apoptosis [10], and/or necrosis [11]. In addition, it has been suggested that ionizing radiation disrupts vascular permeability, which may further exacerbate secondary tissue damage [12].

With the development of medical science, it has been surprising to discover that the pathogenesis and treatment of many diseases are related to the regulation of the immune system, including cardiovascular disease [13], neurodegenerative diseases [14], metabolic diseases [15] and even tumors [16,17]. In the past, the inner ear was mistakenly thought to be an immunologically exempt organ because of the blood labyrinth barrier in the inner ear. At present, it has been found in different types of hearing loss models that external stimulus (e.g., noise [18], genetic mutation [19], aging [20], infection [21], etc.) induce cochlear macrophage activation and aggregation and/or cochlear inflammation. There is evidence that macrophage overactivation and macrophage-associated immune inflammatory response may be a bidirectional process [22], and the specific contribution of this response to auditory cell function is not well defined. In the peripheral auditory system, macrophages are not only associated with cochlear immunity and HC survival [23,24] but also affect cochlear ribbon synapse function [25,26]. However, the association between hearing loss, macrophage changes, and cochlear inflammation remains unclear and conflicting. Not long ago, the work of Liu J et al. [27] attracted our interest. They demonstrated that radiation-induced ototoxicity is associated with inflammatory response and excessive ROS in the cochlea via inhibition of the mTOR signaling pathway, and the cochlea showed elevated levels of IL-6, IL-8 and TNF-α after radiation exposure. The team focused well on cochlear inflammation, but ignored the potential effects of changes in cochlear immune cells.

Therefore, in this study, we first set up an animal model of RISNHL and then observed changes in inner ear morphology, blood and inner ear immune cells, and cochlear inflammation induced by high-dose irradiation. We aim to shed light on the immuno-inflammatory changes in the inner ear following radiation and hope to stimulate the scholars' interest in the immune mechanisms responsible for radiation ototoxicity.

2. Results

2.1. Changes in peripheral immune cells in mice after a single local high dose of ionizing radiation

After a single 30Gy whole head X-ray irradiation (Fig. 1a), the total number of white blood cells, lymphocytes, and intermediate cells (Fig. 1b–d) in the venous blood of the mice was quite sensitive to ionizing radiation and reduced significantly on the first day after exposure. Bone marrow precursors give rise to monocytes in the blood, which circulate for a few days before migrating to the tissues, where they differentiate into different types of macrophages. Cells of this lineage are collectively known as mononuclear phagocytes or monocytes/macrophages. For human and mouse blood monocytes, a division into three subsets, classical, intermediate, and

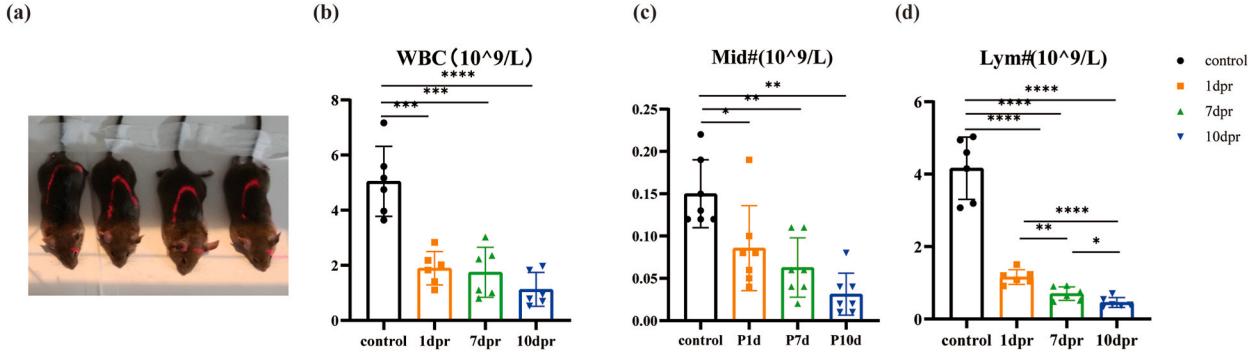

Fig. 1. Radiation model and peripheral immune cell changes in mice. (**a**) Irradiation of the mouse cochlea (the yellow light area is the irradiation exposure area) (**b**)–(**d**) Changes in white blood cells (WBC#), intermediate cells (Mid#), and lymphocytes (Lym#) in peripheral blood of mice after radiation exposure. (n = 6 in each group). (For interpretation of the references to color in this figure legend, the reader is referred to the Web version of this article.)

nonclassical, has been proposed [28]. Intermediate cells are thought to represent a transitional state in the differentiation and maturation of monocytes. The number of cells decreases with increasing observation time. The WBC count of the control group, 1-day post-radiation (1dpr), 7-days post-radiation (7dpr), and 10-days post-radiation (10dpr) was 5.05 ± 1.27 10^9/L, 1.9 ± 0.61 10^9/L, 1.75 ± 0.91 10^9/L, and 1.13 ± 0.61 10^9/L, respectively. The WBC was reduced in all irradiated groups compared to the control group. The intermediate cell counts of the control, 1dpr, 7dpr, and 10dpr groups were 0.16 ± 0.04 10^9/L, 0.09 ± 0.06 10^9/L, 0.06 ± 0.04 10^9/L, and 0.02 ± 0.01 10^9/L, respectively, and all of the experimental groups had a significantly lower cell count than the control group. The absolute values of lymphocytes in the control, 1dpr, 7dpr, and 10dpr groups were 4.16 ± 0.86 10^9/L, 1.16 ± 0.2 10^9/L, 0.70 ± 0.19 10^9/L, and 0.46 ± 0.14 10^9/L, respectively. All exposure groups were significantly lower than the control group, and the number of cells decreased with time after exposure. In summary, these results suggest that high doses of radiation induce a systemic response. Immune cells in the peripheral blood of the mice were so sensitive to the radiation and were inhibited for a short time.

2.2. *Changes in cochlear macrophages and inflammatory mediators in mice after high-dose irradiation*

Cochlear macrophages and nuclei were labeled with GFP (green) and DAPI (blue) immunofluorescence, respectively, and the number of cochlear macrophages decreased after noise exposure (Fig. 2a). In the apical basilar membrane, the number of macrophages significantly declined in the 1dpr, 7dpr, and 10dpr groups compared to the control group with statistical significance ($F = 80.63$, $p < 0.0001$, $n = 12$). The number of macrophages in the 7dpr and 10dpr groups was significantly lower than that in the 1dpr group. There was no significant difference in the number of macrophages between the 7dpr group and 10dpr groups (Fig. 2b); in the middle turn of the basilar membrane (Fig. 2c), the number of macrophages decreased significantly in the three irradiated groups with statistical

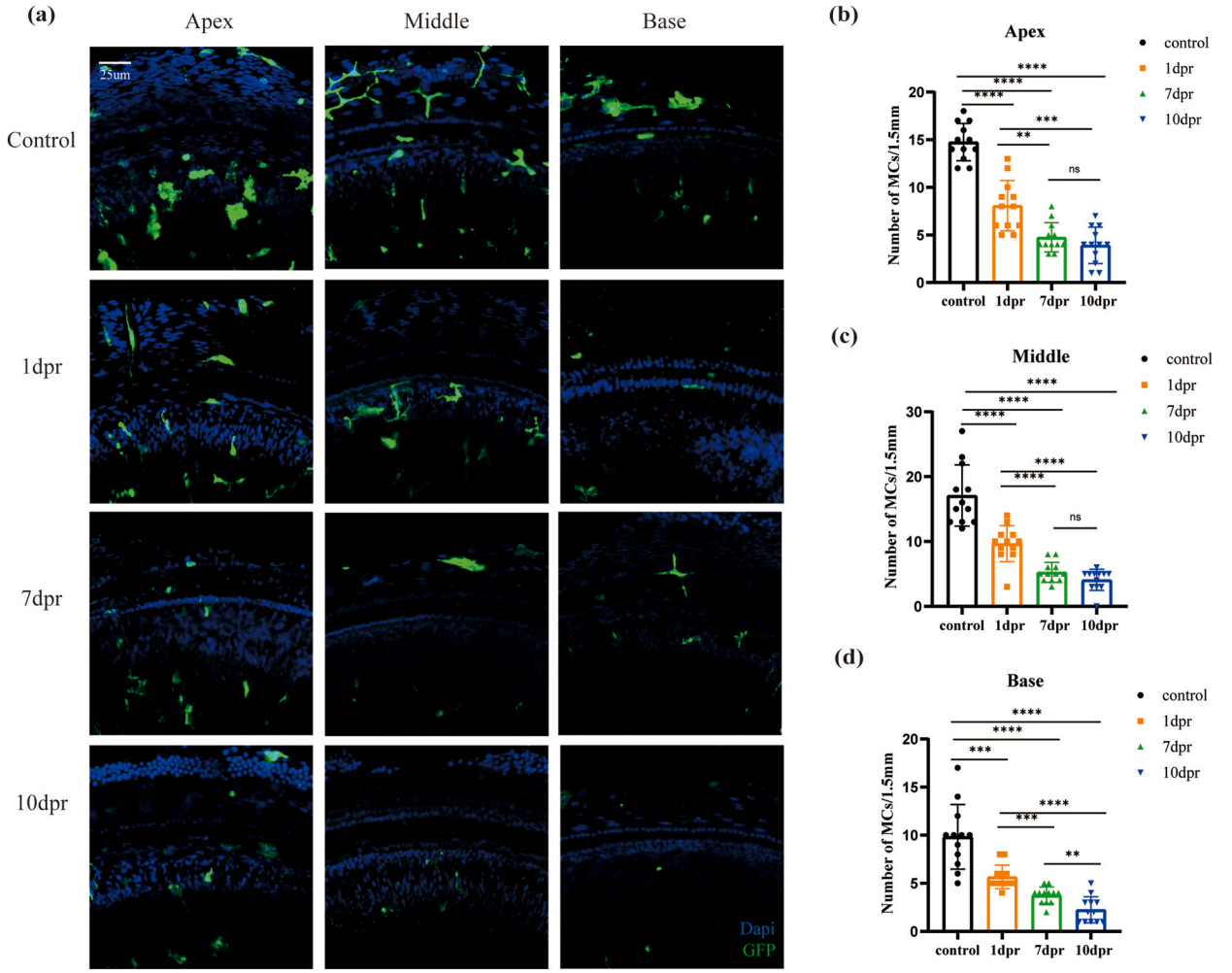

Fig. 2. Cochlear macrophages gradually decline after exposure to ionizing radiation. (a) Macrophages in the cochlear basilar membrane (blue DAPI, green GFP, 40 × magnification). (b)–(d) The number of macrophages following irradiation. (n = 12 in each group). (For interpretation of the references to color in this figure legend, the reader is referred to the Web version of this article.)

significance ($F = 42.38$, $p < 0.0001$, $n = 12$). The trends of the statistical analyses between the three experimental groups were comparable to those observed in the apical turn. In the basal turn (Fig. 2d), the macrophage population decreased in a time-dependent manner ($F = 39.35$, $p < 0.0001$, $n = 12$).

The expression of inflammatory factors IL-1β, IL-6, TNF-α, and chemokines CCL2, CCL3, and CCL4 in the cochlea was quantitatively assessed by RT-qPCR. The results showed that IL-1β, IL-6, TNF-α, and CCL2 increased significantly at 1dpr. IL-1β, TNF-α, and CCL2 then showed a decreased trend with time (Fig. 3). IL-6, CCL3, and CCL4 showed a similar pattern of "rapid up-regulation followed by slow down-regulation", but the observed changes in expression did not reach statistical significance.

Together, these findings indicate that macrophages in the basilar membrane region of the cochlea are sensitive to radiation and decrease significantly with time after radiation exposure. At the same time, inflammatory mediators in the cochlea increased rapidly after irradiation and then downregulated.

2.3. Mice exposed to high doses of radiation showed impaired hearing function without hair cell loss in the short term

The ABR hearing test is commonly used to assess the function of the auditory pathway from the cochlea to the brainstem in mice. In our experiment, compared to the pre-irradiation period, the click thresholds in mice (Fig. 4a) remained relatively stable for 7-days after irradiation. However, a significant threshold increase was observed on day 10th post-irradiation ($t = 10.30$, $p = 0.0001$, $n = 6$). Statistical analysis was performed on the click ABR I wave latency (Fig. 4b) and amplitude (Fig. 4c) of the mice. Similarly, no statistically significant difference was found between the 1dpr and 7dpr groups. However, the latency in the 10dpr group was found to be longer than that observed before irradiation ($t = 3.973$, $p = 0.0106$, $n = 6$), while the amplitude was found to have decreased in the 10dpr group ($t = 7.023$, $p = 0.0009$, $n = 6$). The latency and amplitude of the ABR-I wave at all frequencies in each group were statistically analyzed. The results showed that the latency of the ABR-I wave in the 1dpr and 7dpr groups did not exhibit significant changes at any frequency compared to the pre-irradiation period. However, the latency of the ABR-I wave was prolonged in the 10dpr group, accompanied by a statistically significant decrease in amplitude (Fig. 4e–j).

The hair cell cilia and nucleus were labeled with phalloidin (red) and DAPI (blue) under confocal laser microscopy. The entire segment of the basilar membrane was observed and captured under a 10 × objective lens for counting the hair cells Representative regions of the basilar membrane's apical, middle, and basal turns were captured at 40 × magnification (Fig. 5a). No significant hair cell

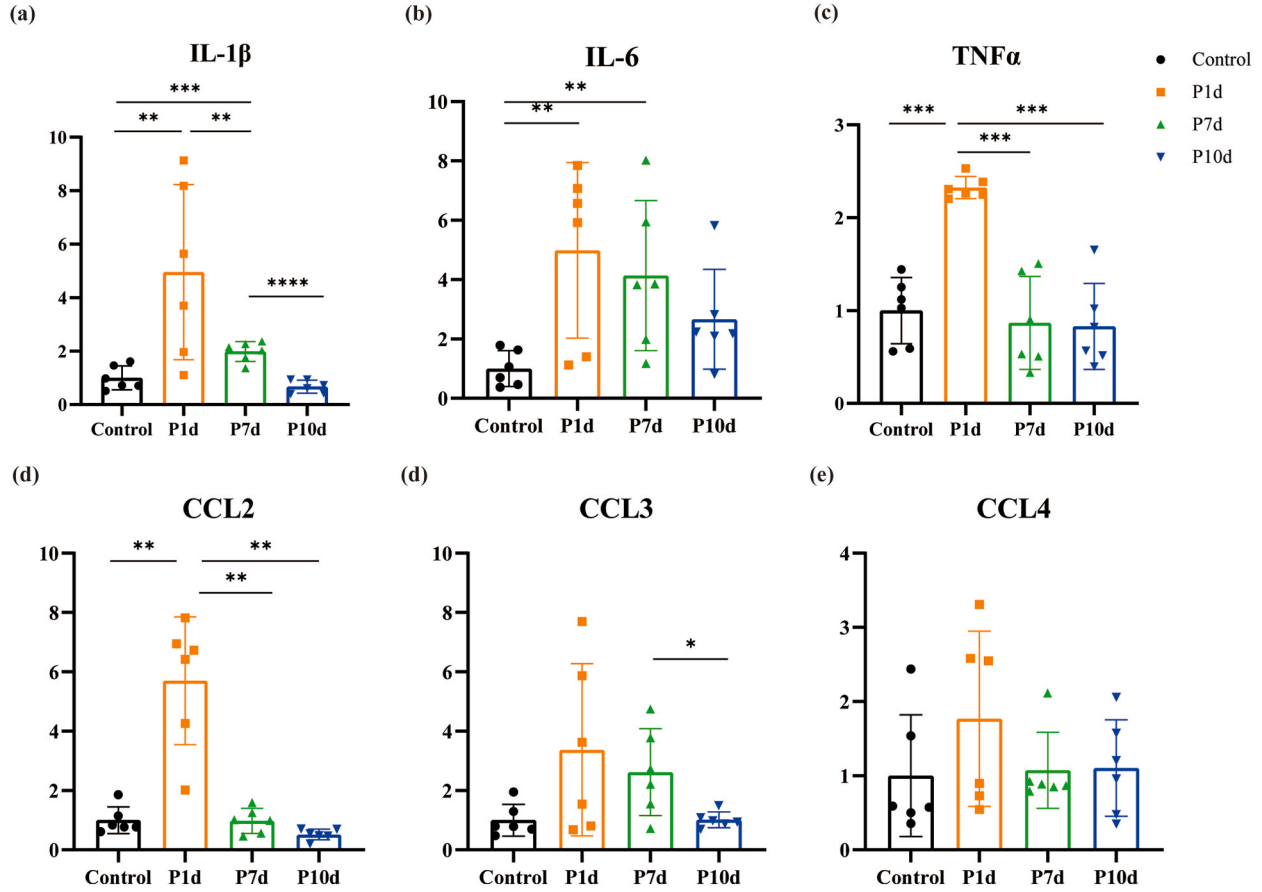

Fig. 3. Changes in inflammatory mediators in the inner ear following irradiation. (n = 6 in each group).

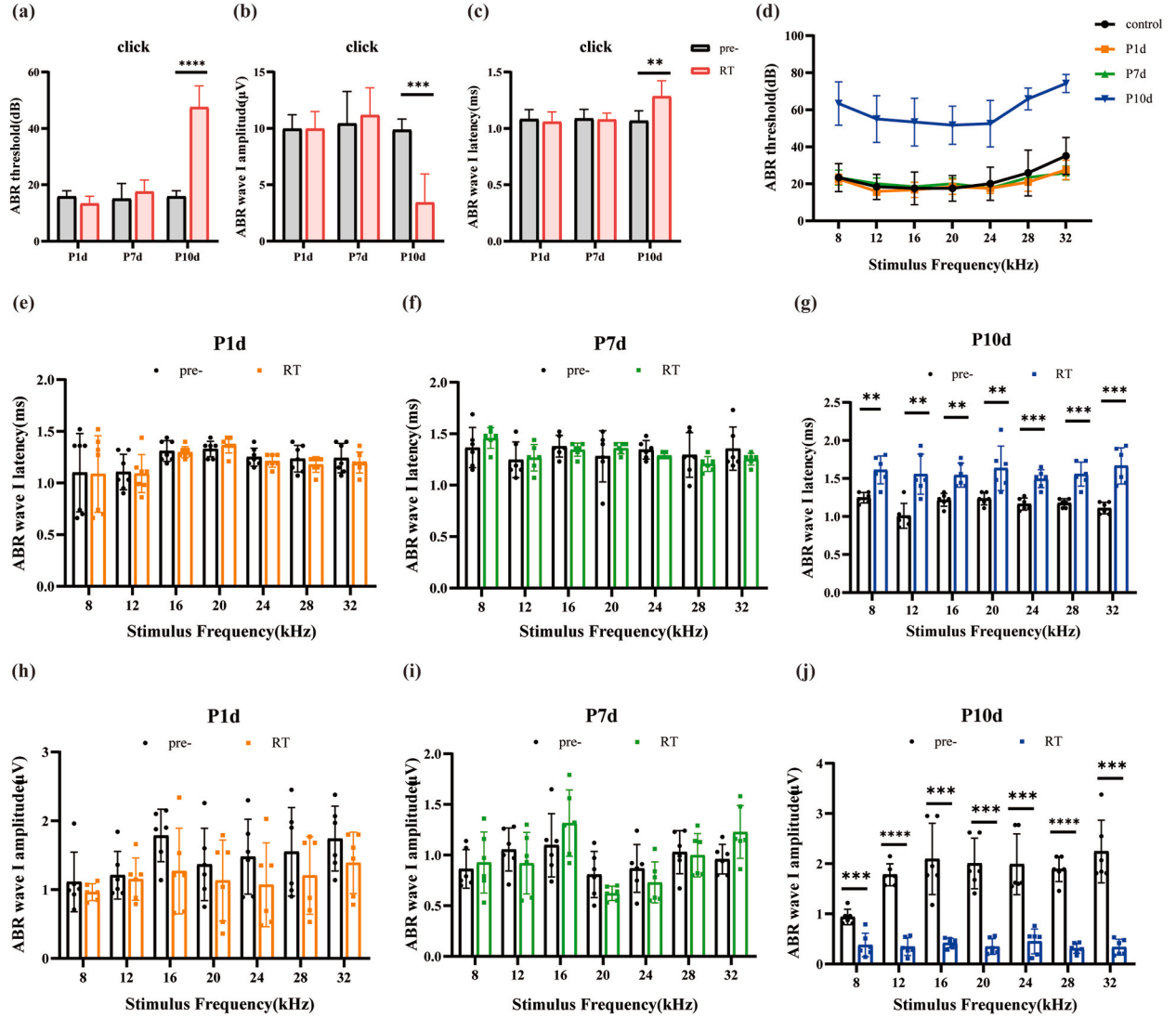

Fig. 4. The effects of ionizing radiation on hearing in mice. (a)–(c) Changes in click threshold, I-wave amplitude, and I-wave latency. (d) Changes in ABR threshold at different frequencies. (e)–(g) Changes in I-wave latency at different frequencies. (h)–(j) Changes in I-wave amplitude at different frequencies.

loss was observed in the irradiated group, and there was no decrease in outer hair cell survival compared to the control group (Fig. 5b–d).

Taken together, these data reveal that the acute phase of high-dose irradiation resulted in pantonal hearing loss in mice without hair cell loss.

2.4. High-dose irradiation-induced morphological changes in SGN

HE staining of cochlear sections revealed that SGN cells in the inner ear of mice exhibited morphological changes on day 10th after irradiation (Fig. 6a–d). Compared with the control group, cells in the SGN and modiolus regions of the cochlea in the 10dpr group showed deeper staining, accompanied by a reduction in interstitial tissue. However, the density of cell distribution remained largely unaltered at low magnification. At high magnification, however, some of the nuclei in the SGNs are knotted and more deeply stained (arrows), and the whole cell is spindle-shaped. Immunofluorescence staining of neurofilaments showed that the protein fluorescence intensity in the apex, middle, and base SGN and the central axis of the cochlea was significantly lower in the 10dpr group than in the control group (Fig. 6e).

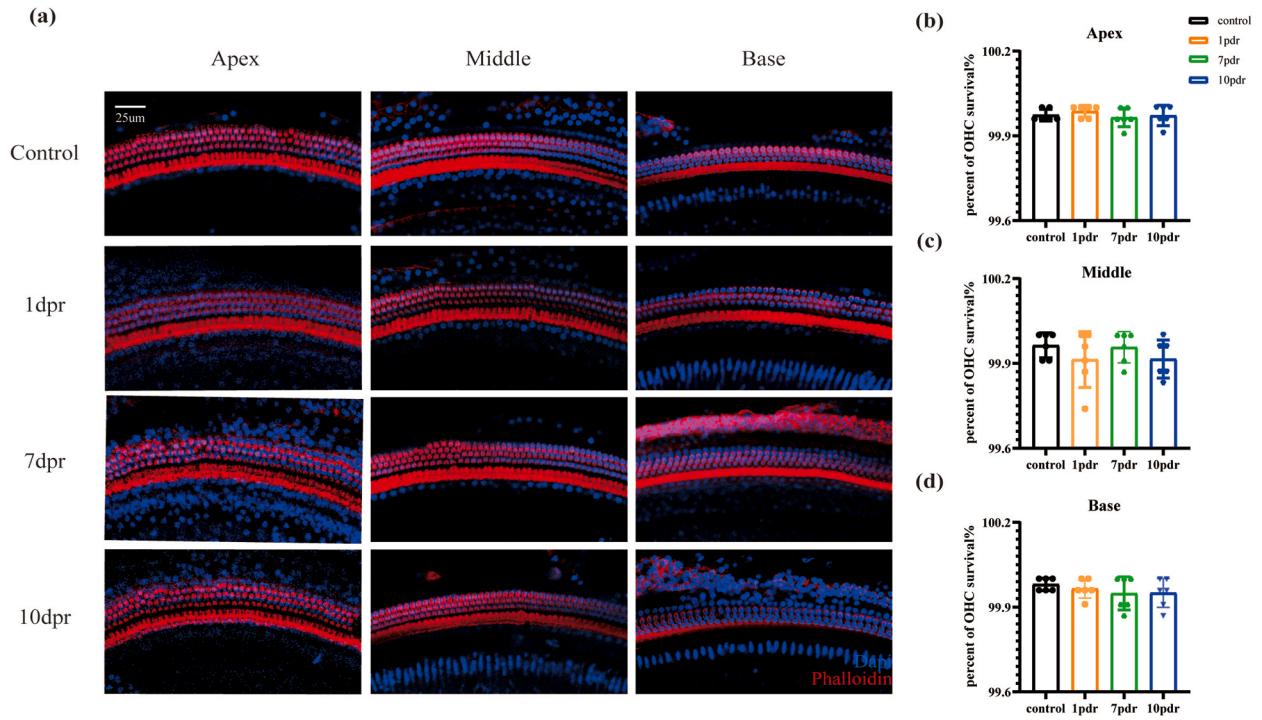

Fig. 5. Hair cells in the inner ear were not damaged after irradiation. (a) Hair cells in the cochlear basilar membrane (blue DAPI, red phalloidin, 40 × magnification) (b)–(d) The number of hair cells following irradiation. (n = 6 in each group). (For interpretation of the references to color in this figure legend, the reader is referred to the Web version of this article.)

3. Discussion

In our study, there was no change in the ABR threshold during the first week post-radiation after the 30Gy X-ray exposure. However, in the 10dpr group, the ABR threshold increased significantly for all tested frequencies, accompanied by a prolonged latency and a down-regulated amplitude of the ABR I wave. At the same time, a single high-dose cranial irradiation did not cause hair cell loss in the basilar membrane within 10-days of irradiation. Nonetheless, morphological changes in the SGN and reduced expression of neurofilaments were found in the cochlea. Finally, the number of cochlear macrophages and peripheral immune cells decreased dramatically over time after irradiation. However, the expression of proinflammatory mediators in the cochlea showed a trend of increase and then decrease.

Our high-dose radiation model showed an acute pantonal hearing loss, and the results suggested that acute RISNHL may not be attributable to cochlear hair cell death. To our surprise, we discovered the morphological changes in both SGNs and neurofilaments. Our results are at odds with many previous studies highlighting the loss of hair cells after irradiation. As early as 1980, low doses of cranial irradiation were found to be safe for the auditory system [29], while high doses of radiation caused hair cell and SGN degeneration [30]. Keilty, Dana et al. proposed that a mean cochlea dose of $\leq$30 Gy is proposed as a means of reducing the risk of HL [5]. Several researchers have proposed that the hair cell loss at the basal turn of the basilar membrane is significantly higher at the apex. This would explain that preferential hearing loss occurs preferentially in the high-frequency region and then slowly moves towards the low-frequency regions [3,5,27,31,32]. Specific conditions of irradiation, including the age of the animal, the type of radiation, the irradiated area, the irradiation dose, and the time after irradiation, may result in disparate experimental outcomes (as shown in Table 1 in the supplementary material). This may partly explain why our study differs from others. Our experiments surprisingly found that SGNs exhibit morphological changes after irradiation. In contrast to the control group, the nuclei of the SGN showed a knotted and darker coloration, while the cell morphology was spindle-shaped in mice exposed to radiation. These morphological features may be indicative of cellular atrophy, a pathological process. However, further exploration of the cellular function underlying morphological changes is still needed. Also, we found that neurofilament protein expression was downregulated in the SGN region. Neurofilaments provide structural support for highly asymmetric neuronal geometries and are essential for efficient neural conduction velocities [33,34]. Previous studies have also shown that ionizing radiation can rapidly cause neurofilament aggregation and reduced nerve fiber density, impairing auditory neural synchronization [34–38]. Our results are partly consistent with a small number of previous studies, which have demonstrated that the initial impact of short-term post-exposure focuses on spiral ganglion cell bodies [39] and ribbon synapses [40], resulting in a significant threshold shift for irradiation dosages $\geq$20 Gy. Consequently, changes in SGN cells and downregulation of neurofilament expression induced by high-dose irradiation may have some potential relevance to radiation-induced hearing loss. Nonetheless, this hypothesis is not well supported by sufficient evidence.

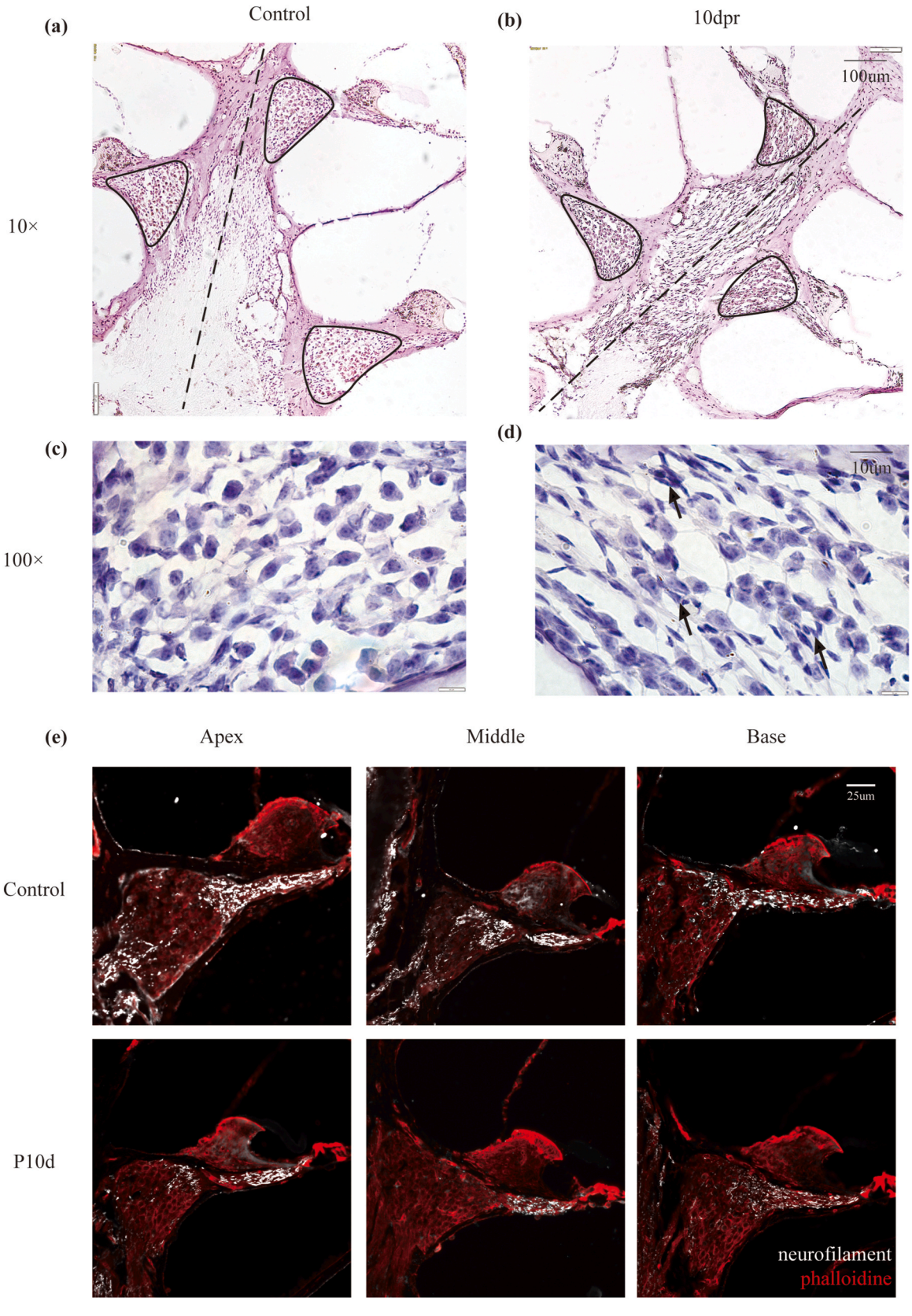

(caption on next page)

Fig. 6. Morphological changes in SGNs induced in the cochlea by ionizing radiation. (a)–(b) HE staining of cochlear axial sections (10 × magnification). The black dotted line shows the cochlear axis and the black curve circles the cochlear SGN region. (c)–(d) HE staining of the SGN area in a cochlear axial section (100 × magnification). Black arrows indicate representative morphological changes observed in the cells following radiation exposure. (d) Immunofluorescence staining of neurofilaments in the SGN area of a cochlear section (red: phalloidin; white: neurofilaments. 40 × magnification). (For interpretation of the references to color in this figure legend, the reader is referred to the Web version of this article.)

Under our experimental conditions, irradiation did not result in significant loss of cochlear hair cells. This phenomenon is related not only to the irradiation conditions but also to the physical principles of ionizing radiation. It has been demonstrated that ionizing radiation can directly cause DNA damage, cell death, and disruption of tissue function [10,41,42]. Cell cycle regulation is the most important factor influencing cellular sensitivity to ionizing radiation, and cells exhibit maximum radiosensitivity in the G (2)-M phase [43]. Proliferating and dividing active cells, such as malignant tumor cells and stem cells, are primarily in phase M of the cell cycle. As a result, they are very sensitive to radiation, a fundamental principle of radiotherapy. In contrast, terminally differentiated cells lose their ability to divide, making them insensitive to radiation, such as neurons and myocytes [44]. Mammalian inner ear hair cells are highly differentiated mature cells that cannot divide [45] and are therefore insensitive to radiation. It is noteworthy that in some studies, chronic hair cell loss induced by low/moderate dose irradiation may be a manifestation of the “bystander effect” [46,47]. Our study was limited to results obtained within 10 days after a single 30 Gy X-ray cranial irradiation of CBA/J mice. Thus, the immediate direct effect of radiation is greater than the chronic bystander effect. This may explain why high-dose irradiation does not readily result in the death of highly differentiated hair cells.

In the present study, high-dose cranial irradiation of CBA/J mice resulted in myelosuppression [48], accompanied by a dramatic reduction in cochlear macrophages and alterations in the immune microenvironment of the inner ear. Our previous studies have shown that macrophages are major cells involved in the immune response in the inner ear, as well as in the structures that make up the blood labyrinth barrier [18]. Previous studies in the noise-induced hearing loss [18,49] model and the connexin26-deficiency hearing loss model [19] have shown that the death of hair cells and SGNs is accompanied by an increase in the number of inner ear macrophages. These macrophages may be involved in cochlear damage and hearing loss through modulation of cochlear inflammation. It has been demonstrated that noise-induced hearing loss or connexin26-deficiency hearing loss can be preserved using the macrophage inhibitor clodronate liposome [49] or the anti-inflammatory agent dexamethasone [50], respectively. However, in this experiment, we showed for the first time that cochlear macrophages are significantly reduced in the radiation-induced hearing loss model. This finding is similar to several previous in vitro studies investigating the effects of irradiation on macrophages [51,52]. Also, our irradiation model showed the rapid up-regulation of inner ear IL-1β, IL-6, TNF-α, and CCL2, suggesting that high-dose cranial irradiation may induce M1-type macrophage-associated immune response [53,54]. In general, low-dose irradiation tends to promote macrophage polarization towards the anti-inflammatory M2 phenotype, whereas high-dose irradiation tends to promote macrophage polarization patterns towards the pro-inflammatory M1-like phenotype and induces harmful bystander effects, including neuroinflammation and upregulation of the pro-inflammatory factors IL-1β, IL-6, CCL2, and TNF-α [55–57], which has been confirmed in CBA/J mice [58]. In addition, we sought to explain the relationship between RISNHL and immunosuppression, so we had assumed that immunosuppression would make the body more susceptible to infections, including otitis, which can also cause pantonal hearing loss [21]. However, we found no evidence of middle ear inflammation, such as empyema in the cochlea, in the cochlear anatomy of the animal. Consequently, we speculated that high-dose irradiation may directly kill cochlear macrophages and block the chemotactic recruitment of circulating macrophages to the inner ear. But, the relationship between irradiation-induced immune changes and hearing loss remains to be explored.

In summary, the present study is a suitable model for acute RISNHL. Our findings suggest that localized high-dose irradiation results in systemic immune cell inhibition, alteration of inner ear morphology, and changes in the cochlear immune microenvironment. However, the results of this experiment are largely descriptive, and the relationship between post-irradiation auditory function, morphological changes in the inner ear, auditory-related nerve cells and conduction pathways, and immune responses in the inner ear needs further exploration. Inflammation of the inner ear is closely related to hair cell survival and cochlear function [59,60]. In models of hearing damage induced by multiple stimuli (including noise [26,49], infection [21,23], genetic mutation [19,24], etc. [25,26]), early modulation of immune cells or inflammatory responses contributes to hearing protection. In the RISNHL model, only a few studies have been performed to protect hearing by intervening in the oxidative stress response [27]. Therefore, as a next step, we need to clarify the role that cochlear macrophage-associated immune responses play in modulating the auditory pathway (from sensory epithelium to auditory cortex) and explore protective measures. Furthermore, based on the high sensitivity of the cochlear vascular endothelium to irradiation [61,62], it would be a good direction of research to find out whether perivascular macrophage-like melanocytes, which are a component of the blood labyrinth barrier [63], are suppressed by radiation (as demonstrated in the present experiments) and lead to inner ear lesions [64].

4. Limitations of the study

SNHL induced by high doses of radiation is not associated with hair cell loss but rather with morphological changes in SGN cells. Short-term RISNHL is accompanied by a significant reduction in cochlear macrophages and changes in the immunological microenvironment. However, the underlying mechanisms between these findings remain to be investigated. In addition, we did not explore protective measures against RISNHL.

5. Star methods

5.1. Key resources table

Please refer to the "supplementary material" section.

5.1.1. Resource availability

Lead contact Further information and requests for resources and reagents should be directed to and will be fulfilled by the lead contact, Sun Yu (sunyu@hust.edu.cn).

Materials availability This study did not generate new unique reagents.

5.2. Experimental model and subject details

5.2.1. Animals

In this study, 8-week-old male Cx3cr1$^{GFP/+}$ heterozygous mice were bred in-house on a CBA/J background. The GFP gene replaces one allele of CX3CR1, a fractalkine receptor. Cx3cr1 is expressed in macrophages, monocytes, microglia, NK cells, and related cells [26]. As a result, Cx3cr1$^{GFP/+}$ mice can express GFP in all macrophages, making it easier to track the number and location of macrophages in the interior of the body. Auditory brainstem response (ABR) tests were performed on all mice before the experiment to ensure that they had good hearing. All the mice were bred in the SPF animal room of the laboratory animal center of Tongji Medical College, Huazhong University of Science and Technology. The operator holds the certificate of laboratory animal professional technical examination.

48 healthy mice with good hearing were divided into four groups of 12 mice each: control, 1dpr, 7dpr, and 10dpr. All irradiated groups were exposed to 30Gy of X-rays and ABR hearing tests were performed at the time of observation, after which they were killed under anesthesia and samples were collected. In the control group, ABR hearing tests were measured and samples were collected at the same time as in the irradiated group. The control group was matched to the experimental group for all treatments except irradiation. In addition, the control animals were placed on a radiotherapy table for the same amount of time after anesthesia, but without the radiation dose. Six mice from each group were randomly selected for peripheral blood sampling. The basilar membrane of one cochlea was dissected and the other cochlea was used for frozen sections. In the remaining six mice, one side of the cochlea was retained for RNA extraction, and the basilar membrane of the other side was also dissected for morphological study.

5.2.2. Radiation exposure

Mice were anesthetized with Zoletil 50 (30 mg/kg, Virbac, Fronce) and Xylazine (10 mg/kg, LGM Pharma, America) by intraperitoneal injection. The irradiation field was adjusted to 8 cm × 40 cm covering the skull of the mice. The distance from the source axis to the shaft was 100 cm and the thickness of the lead block was 10 cm [27]. Mice were irradiated with a single dose of 30 Gy using 6-MV X-rays (600 MU min−1, Trilogy System Linear Accelerator, Varian Medical Systems) [27].

6. Method details

6.1. Auditory brainstem response

After deep anesthesia, the mice were placed in a thermostatic blanket to maintain body temperature during the measurement. Three electrode pins were placed, the reference electrode was inserted under the skin of the mastoid of the test ear (reversed electrode), the recording electrode was inserted under the skin of the median skull base of the mouse (simultaneous electrode), and the common electrode was inserted under the skin of the mastoid of the opposite ear (grounded). The computer's TDT system was switched on to generate the stimulus tone, which was amplified by the device and transmitted to a speaker and then to the ear, where the evoked potential was sent to a signal processor in the computer for superposition processing. The stimuli were Click and short pure tones at 8 kHz, 12 kHz, 16 kHz, 20 kHz, 24 kHz, 28 kHz, and 32 kHz with a repetition rate of 10 per second, a scan time of 10 ms, and a superposition of 512 times. The sound intensity of the test starts at 80 dB SPL and gradually decreases by 5 dB SPL as it approaches the threshold, which is represented by the sound intensity of the ABR I wave in the visually detectable brainstem potential wave group [65]. The ABR wave I is proposed to represent the summed action potentials of the auditory nerve fibers. The amplitude is determined as the value from the baseline to the first peak, while the latency is determined as the time at which this peak occurs. To avoid subjective differences, the results were read by one person and the raters were blinded to the experimental conditions [40].

6.2. Blood sample and cochlear acquisition

Under anesthesia following the ABR test, the mice's eyeballs of the mice were quickly removed and we collected blood from the retroorbital venous plexus. The blood was collected in a glass tube prefilled with anticoagulant until the bleeding stopped. A TEK-VET3 automatic blood cell analyzer was utilized for blood analysis. WBC reference interval (0.8–6.8) × 10^9/L, Lym# reference interval (0.7–5.7) × 10^9/L, and Lym% reference interval 55.8%–90.6 % were used in mice. Mice were then killed by cervical dislocation, and the cochlea was carefully detached from the temporal bone and placed in pre-cooled, fresh 4 % paraformaldehyde. The circular and oval windows of the cochlea were opened under a microscope, and the cochlea was flushed with an infusion of paraformaldehyde with

a needle to whited the cochlea. The cochlea was placed in 4 % paraformaldehyde in a refrigerator at 4 °C overnight.

6.3. Hematoxylin-eosin (HE) staining

The cochlear section was immersed in PBS solution for 10 min for cutting temperature compound (OCT), 3 min for hematoxylin, and washed with tap water for 30 s. It was immersed in 1 % ethanol for 2 s, stained with eosin for 4 min, immersed in 95 % ethanol for 2 min, immersed in anhydrous ethanol for 2 min, cleared in xylene for 10 min, and sealed with neutral glue.

6.4. Immunofluorescence staining

The fixed cochlea was decalcified in a 10 % EDTA solution for 24 h. For frozen sections, the cochlea was dehydrated in 10 %, 20 %, and 30 % sucrose solutions for 1 h, respectively, and embedded in optimal OCT at 4 °C overnight. A 10 mm section of the medial axis of the cochlea was removed for subsequent experiments. For basilar membrane placement, each cochlea was carefully dissected in 0.01 M of frozen PBS. Cochlear sections or basilar membrane products were incubated in a blocking solution (10 % donkey serum plus 0.1 % Triton X-100) for 1 h at room temperature. The samples were then incubated with rabbit polyclonal anti-GFP antibody (1:200 dilution, M048-3, MBL, Beijing, China) to enhance green fluorescence of macrophage or anti-neurofilament heavy chain antibody (1:500 dilution, AB5539, Sigma-Aldrich, America) at 4 °C overnight. The samples were washed 3 times in 0.01 M PBS containing 0.1 % Tween-20 and then stained with Alexa Fluor 647 donkey anti-rabbit IgG (1:200 dilution, ANT032, Antgene, China) or Alexa Fluor 488 Donkey Anti-Chicken IgY (1:200 dilution, A78948, Thermo Fisher Scientific, America) for 2 h. DAPI (C1005, Beyotime Biotechnology) and phalloidin (0.05 mg/ml, P5282, Sigma-Aldrich) were used for nuclear and F-actin staining. Images were obtained by laser scanning confocal microscopy (Nikon, Tokyo, Japan). Macrophages were visualized by GFP immunostaining.

6.5. Cell count

The basilar membrane was scanned and reconstructed under a 10 × mirror. Measure the length of the basilar membrane using the "measure line" tool in ImageJ software. Count the number of inner hair cells using the length of 100um as the unit of measurement. Under normal circumstances, the number of outer hair cells should be inner hair cells × 3. At the same time, the number of missing outer hair cells was counted, and finally, 1.5 mm was removed from each segment (apex, middle, and base) of the basilar membrane. Outer hair cell survival rate = (1- total number of missing outer hair cells/number of inner hair cells × 3) × 100 %. The region between the inner hair cells and the third row of outer hair cells is the sensory neuroepithelial region where we count macrophages.

6.6. RNA preparation and real-time quantitative polymerase chain reaction

RT-qPCR detected the transcriptional expression levels of the following genes: TNF-α, IL-1β, IL-6, CCL2, CCL3, and CCL4. After the animal was killed and the cochlea removed, the connective tissue surrounding the cochlea was quickly removed in a pre-cooled PBS buffer and then placed on ice for RNA extraction. One cochlea was used as a sample and six biological replicates were performed for each experimental condition. Total RNA was extracted from the collected tissues using FastPure Cell/Tissue Total RNA Isolation Kit V2 (Vazyme. Nanjing, China). Reverse transcription was performed using HiScript III 1st Strand cDNA Synthesis Kit (+gDNA wiper) (Vazyme. Nanjing, China). RT-qPCR was performed on the Roche LightCycler 480 instrument using the SYBR green PCR technique. The relative gene expression data of each group were analyzed by the standard $2^{-\triangle ct}$ method. The following primers were used for RT-qPCR:

GAPDH Forward GCCAAGTATGATGACATCAAGAAGG.
GAPDH Reverse GCTGTAGCCGTATTCATTGTCATAC.
IL-1β Forward GAAATGCCACCTTTTGACAGTG.
IL-1β Reverse TGGATGCTCTCATCAGGACAG.
IL-6 Forward AATTTCCTCTGGTCTTCTGGAGTAC.
IL-6 Reverse GACTCCAGCTTATCTGTTAGGAGAG.
TNFα Forward CAGGCGGTGCCTATGTCTC.
TNFα Reverse CGATCACCCCGAAGTTCAGTAG.
CCL3 Forward GCAACCAAGTCTTCTCAGCG.
CCL3 Reverse TCTCTTAGTCAGGAAAATGACACC.
CCL4 Forward TGTGCAAACCTAACCCCGAG.
CCL4 Reverse GGGTCAGAGCCCATTGGTG.
CCL2 Forward TAAAAACCTGGATCGGAACCAAA.
CCL2 Reverse GCATTAGCTTCAGATTTACGGGT.

6.7. Statistical analysis

Statistics were performed using GraphPad Prism 8.0 (GraphPad Software Inc., La Jolla, CA, USA) and IBM SPSS Statistics 21.0 (SPSS Inc., Chicago, IL, USA). All values in the figures are presented as mean ± standard deviation (SD). For three or more groups, we first performed a factorial ANOVA analysis. For a P value < 0.05, we then used t-tests to compare pairs of subgroups. The independent

samples *t*-test was used to compare the mean between the two groups, and the paired samples *t*-test was used to compare the mean between the self-controlled samples. $P < 0.05$ was considered statistically significant.

Data availability statement

All data included in this study are available upon reasonable request by contact with the corresponding author.

Ethics statement

All animal experimental operations complied with the "Guidelines for the Care and Use of Experimental Animals" issued by the NIH of America, and were approved by the Experimental Animal Ethics Committee of Tongji Medical College, Huazhong University of Science and Technology (Approval No. 3638).

CRediT authorship contribution statement

Mengwen Shi: Writing – original draft, Investigation. **Ye Wang:** Resources, Investigation, Data curation. **Huiwen Yang:** Investigation, Data curation. **Chengcai Lai:** Validation, Methodology, Formal analysis. **Jintao Yu:** Writing – review & editing, Validation, Data curation, Conceptualization. **Yu Sun:** Writing – review & editing, Supervision, Funding acquisition, Conceptualization.

Declaration of competing interest

The authors declare that they have no known competing financial interests or personal relationships that could have appeared to influence the work reported in this paper.

Acknowledgments

We particularly thank KunYu Yang for his advice and suggestions on the radiation method. We are grateful to the cancer center (Wuhan Union Hospital) for their guidance and assistance with the radiation. This work was supported by the Innovative Research Groups of Hubei Province (No. 2023AFA038), the National Natural Science Foundation of China (No. 82071058), the Fundamental Research Funds for the Central Universities (Grant No. YCJJ20230111), and the National Key Research and Development Program of China (No. 2021YFF0702303).

Appendix A. Supplementary data

Supplementary data to this article can be found online at https://doi.org/10.1016/j.heliyon.2024.e37223.

References

[1] X. Wang, C. Hu, A. Eisbruch, Organ-sparing radiation therapy for head and neck cancer, Nat. Rev. Clin. Oncol. 8 (2011) 639–648, https://doi.org/10.1038/nrclinonc.2011.106.
[2] E.M. Lambert, G.B. Gunn, P.W. Gidley, Effects of radiation on the temporal bone in patients with head and neck cancer, Head Neck 38 (2016) 1428–1435, https://doi.org/10.1002/hed.24267.
[3] M.A. Mujica-Mota, S. Lehnert, S. Devic, K. Gasbarrino, S.J. Daniel, Mechanisms of radiation-induced sensorineural hearing loss and radioprotection, Hear. Res. 312 (2014) 60–68, https://doi.org/10.1016/j.heares.2014.03.003.
[4] A.C. Nichols, J. Theurer, E. Prisman, N. Read, E. Berthelet, E. Tran, et al., Radiotherapy versus transoral robotic surgery and neck dissection for oropharyngeal squamous cell carcinoma (ORATOR): an open-label, phase 2, randomised trial, Lancet Oncol. 20 (2019) 1349–1359, https://doi.org/10.1016/S1470-2045(19)30410-3.
[5] D. Keilty, M. Khandwala, Z.A. Liu, V. Papaioannou, E. Bouffet, D. Hodgson, et al., Hearing loss after radiation and chemotherapy for CNS and head-and-neck tumors in children, J. Clin. Oncol. : Official Journal of the American Society of Clinical Oncology 39 (2021) 3813–3821, https://doi.org/10.1200/JCO.21.00899.
[6] W.J.T. Tan, L. Song, Role of mitochondrial dysfunction and oxidative stress in sensorineural hearing loss, Hear. Res. 434 (2023) 108783, https://doi.org/10.1016/j.heares.2023.108783.
[7] W.-K. Low, M.G.K. Tan, A.W.C. Chua, L. Sun, D.-Y. Wang, 12th Yahya Cohen Memorial Lecture: the cellular and molecular basis of radiation-induced sensorineural hearing loss, Ann. Acad. Med. Singapore 38 (2009) 91–94.
[8] Z. Huang, Y. Wang, D. Yao, J. Wu, Y. Hu, A. Yuan, Nanoscale coordination polymers induce immunogenic cell death by amplifying radiation therapy mediated oxidative stress, Nat. Commun. 12 (2021) 145, https://doi.org/10.1038/s41467-020-20243-8.
[9] H.-Y. Jiang, Y. Yang, Y.-Y. Zhang, Z. Xie, X.-Y. Zhao, Y. Sun, et al., The dual role of poly(ADP-ribose) polymerase-1 in modulating parthanatos and autophagy under oxidative stress in rat cochlear marginal cells of the stria vascularis, Redox Biol. 14 (2018) 361–370, https://doi.org/10.1016/j.redox.2017.10.002.
[10] C. Barrett, I. Hellickson, L. Ben-Avi, D. Lamb, M. Krahenbuhl, K.L. Cerveny, Impact of low-level ionizing radiation on cell death during zebrafish embryonic development, Health Phys. 114 (2018) 421–428, https://doi.org/10.1097/HP.0000000000000788.
[11] W.-Q. Zuo, Y.-J. Hu, Y. Yang, X.-Y. Zhao, Y.-Y. Zhang, W. Kong, et al., Sensitivity of spiral ganglion neurons to damage caused by mobile phone electromagnetic radiation will increase in lipopolysaccharide-induced inflammation in vitro model, J. Neuroinflammation 12 (2015) 105, https://doi.org/10.1186/s12974-015-0300-1.
[12] A. Bouchet, M. Potez, N. Coquery, C. Rome, B. Lemasson, E. Bräuer-Krisch, et al., Permeability of brain tumor vessels induced by uniform or spatially microfractionated synchrotron radiation therapies, Int. J. Radiat. Oncol. Biol. Phys. 98 (2017) 1174–1182, https://doi.org/10.1016/j.ijrobp.2017.03.025.

[13] D. Wolf, K. Ley, Immunity and inflammation in atherosclerosis, Circ. Res. 124 (2019) 315–327, https://doi.org/10.1161/CIRCRESAHA.118.313591.
[14] H.S. Kwon, S.-H. Koh, Neuroinflammation in neurodegenerative disorders: the roles of microglia and astrocytes, Transl. Neurodegener. 9 (2020) 42, https://doi.org/10.1186/s40035-020-00221-2.
[15] G.S. Hotamisligil, Inflammation and metabolic disorders, Nature 444 (2006) 860–867.
[16] J.F.A.P. Miller, M. Sadelain, The journey from discoveries in fundamental immunology to cancer immunotherapy, Cancer Cell 27 (2015) 439–449, https://doi.org/10.1016/j.ccell.2015.03.007.
[17] M.-W. Shi, J. Huang, Y. Sun, Neoadjuvant immunotherapy for head and neck squamous cell carcinoma: expecting its application in temporal bone squamous cell carcinoma, Current Medical Science 43 (2023) 213–222, https://doi.org/10.1007/s11596-023-2700-2.
[18] W. He, J. Yu, Y. Sun, W. Kong, Macrophages in noise-exposed cochlea: changes, regulation and the potential role, Aging and Disease 11 (2020) 191–199, https://doi.org/10.14336/AD.2019.0723.
[19] K. Xu, S. Chen, L. Xie, Y. Qiu, X. Bai, X.Z. Liu, et al., Local macrophage-related immune response is involved in cochlear epithelial damage in distinct gjb2-related hereditary deafness models, Front. Cell Dev. Biol. 8 (2020) 597769, https://doi.org/10.3389/fcell.2020.597769.
[20] H. Lang, K.V. Noble, J.L. Barth, J.A. Rumschlag, T.R. Jenkins, S.L. Storm, et al., The stria vascularis in mice and humans is an early site of age-related cochlear degeneration, macrophage dysfunction, and inflammation, J. Neurosci. : the Official Journal of the Society For Neuroscience 43 (2023) 5057–5075, https://doi.org/10.1523/JNEUROSCI.2234-22.2023.
[21] A. Xia, A. Thai, Z. Cao, X. Chen, J. Chen, B. Bacacao, et al., Chronic suppurative otitis media causes macrophage-associated sensorineural hearing loss, J. Neuroinflammation 19 (2022) 224, https://doi.org/10.1186/s12974-022-02585-w.
[22] P.J. Murray, T.A. Wynn, Protective and pathogenic functions of macrophage subsets, Nat. Rev. Immunol. 11 (2011) 723–737, https://doi.org/10.1038/nri3073.
[23] Y. Hayashi, H. Suzuki, W. Nakajima, I. Uehara, A. Tanimura, T. Himeda, et al., Cochlear supporting cells function as macrophage-like cells and protect audiosensory receptor hair cells from pathogens, Sci. Rep. 10 (2020) 6740, https://doi.org/10.1038/s41598-020-63654-9.
[24] Y. Zhang, X. Fu, Y. Li, W. Li, G. Hong, S. Guo, et al., Macrophage-mediated immune response aggravates hearing disfunction caused by the disorder of mitochondrial dynamics in cochlear hair cells, Hum. Mol. Genet. 32 (2023) 1137–1151, https://doi.org/10.1093/hmg/ddac270.
[25] X. Song, Y. Li, R. Guo, Q. Yu, S. Liu, Q. Teng, et al., Cochlear resident macrophage mediates development of ribbon synapses via CX3CR1/CX3CL1 axis, Front. Mol. Neurosci. 15 (2022) 1031278, https://doi.org/10.3389/fnmol.2022.1031278.
[26] V. Manickam, D.Y. Gawande, A.R. Stothert, A.C. Clayman, L. Batalkina, M.E. Warchol, et al., Macrophages promote repair of inner hair cell ribbon synapses following noise-induced cochlear synaptopathy, J. Neurosci. : the Official Journal of the Society For Neuroscience 43 (2023) 2075–2089, https://doi.org/10.1523/JNEUROSCI.1273-22.2023.
[27] J. Liu, L. Zhu, Y. Bao, Z. Du, L. Shi, X. Hong, et al., Injectable dexamethasone-loaded peptide hydrogel for therapy of radiation-induced ototoxicity by regulating the mTOR signaling pathway, J. Contr. Release : Official Journal of the Controlled Release Society 365 (2023) 729–743, https://doi.org/10.1016/j.jconrel.2023.12.004.
[28] L. Ziegler-Heitbrock, P. Ancuta, S. Crowe, M. Dalod, V. Grau, D.N. Hart, et al., Nomenclature of monocytes and dendritic cells in blood, Blood 116 (2010) e74–e80, https://doi.org/10.1182/blood-2010-02-258558.
[29] G.M. Thibadoux, W.V. Pereira, J.M. Hodges, R.J. Aur, Effects of cranial radiation on hearing in children with acute lymphocytic leukemia, J. Pediatr. 96 (1980) 403–406.
[30] K. Kaga, A. Maeshima, T. Tsuzuku, K. Kondo, T. Morizono, Temporal bone histopathological features of a worker who received high doses of radiation in a criticality accident: a case report, Acta Otolaryngol. 131 (2011) 451–455, https://doi.org/10.3109/00016489.2010.533700.
[31] C. Yang, W. Zhang, X.-L. Liu, Y. Liang, Y.-W. Yuan, C. Ren, et al., Localization of prestin and expression in the early period after radiation in mice, Eur. Arch. Oto-Rhino-Laryngol. : Official Journal of the European Federation of Oto-Rhino-Laryngological Societies (EUFOS) : Affiliated With the German Society For Oto-Rhino-Laryngology - Head and Neck Surgery 271 (2014) 3333–3340, https://doi.org/10.1007/s00405-014-3180-6.
[32] A.P.J. Giese, J.G. Guarnaschelli, J.A. Ward, D.I. Choo, S. Riazuddin, Z.M. Ahmed, Radioprotective effect of aminothiol PrC-210 on irradiated inner ear of Guinea pig, PLoS One 10 (2015) e0143606, https://doi.org/10.1371/journal.pone.0143606.
[33] A. Yuan, M.V. Rao, Veeranna, R.A. Nixon, Neurofilaments and neurofilament proteins in health and disease, Cold Spring Harbor Perspect. Biol. 9 (2017), https://doi.org/10.1101/cshperspect.a018309.
[34] C.T. Dinh, S. Chen, A. Nourbakhsh, K. Padgett, P. Johnson, S. Goncalves, et al., Single fraction and hypofractionated radiation cause cochlear damage, hearing loss, and reduced viability of merlin-deficient schwann cells, Cancers 15 (2023), https://doi.org/10.3390/cancers15102818.
[35] K.A. Irvine, W.F. Blakemore, Remyelination protects axons from demyelination-associated axon degeneration, Brain : J. Neurol. 131 (2008) 1464–1477, https://doi.org/10.1093/brain/awn080.
[36] R.X. Lee, F.R. Tang, Radiation-induced neuropathological changes in the oligodendrocyte lineage with relevant clinical manifestations and therapeutic strategies, Int. J. Radiat. Biol. 98 (2022) 1519–1531, https://doi.org/10.1080/09553002.2022.2055804.
[37] E.B. Masurovsky, M.B. Bunge, R.P. Bunge, Cytological studies of organotypic cultures of rat dorsal root ganglia following X-irradiation in vitro. II. Changes in Schwann cells, myelin sheaths, and nerve fibers, J. Cell Biol. 32 (1967) 497–518.
[38] H. Pan, Q. Song, Y. Huang, J. Wang, R. Chai, S. Yin, et al., Auditory neuropathy after damage to cochlear spiral ganglion neurons in mice resulting from conditional expression of diphtheria toxin receptors, Sci. Rep. 7 (2017) 6409, https://doi.org/10.1038/s41598-017-06600-6.
[39] K.L. Gasser Rutledge, K.G. Prasad, K.R. Emery, A.A. Mikulec, M. Varvares, M.A. Gratton, Short-term peripheral auditory effects of cranial irradiation: a mouse model, Ann. Otol. Rhinol. Laryngol. 124 (2015) 903–910, https://doi.org/10.1177/0003489415591205.
[40] Z. Liu, Y. Luo, R. Guo, B. Yang, L. Shi, J. Sun, et al., Head and neck radiotherapy causes significant disruptions of cochlear ribbon synapses and consequent sensorineural hearing loss, Radiother. Oncol. 173 (2022) 207–214, https://doi.org/10.1016/j.radonc.2022.05.023.
[41] L. Hu, X. Yin, Y. Zhang, A. Pang, X. Xie, S. Yang, et al., Radiation-induced bystander effects impair transplanted human hematopoietic stem cells via oxidative DNA damage, Blood 137 (2021) 3339–3350, https://doi.org/10.1182/blood.2020007362.
[42] I. Mittra, U. Samant, S. Sharma, G.V. Raghuram, T. Saha, P. Tidke, et al., Cell-free chromatin from dying cancer cells integrate into genomes of bystander healthy cells to induce DNA damage and inflammation, Cell Death Discovery 3 (2017) 17015, https://doi.org/10.1038/cddiscovery.2017.15.
[43] T.M. Pawlik, K. Keyomarsi, Role of cell cycle in mediating sensitivity to radiotherapy, Int. J. Radiat. Oncol. Biol. Phys. 59 (2004) 928–942.
[44] J.A. Coffman, Cell cycle development, Dev. Cell 6 (2004) 321–327.
[45] A.S. Edge, Z.-Y. Chen, Hair cell regeneration, Curr. Opin. Neurobiol. 18 (2008) 377–382, https://doi.org/10.1016/j.conb.2008.10.001.
[46] J.H. Pyun, S.U. Kang, H.S. Hwang, Y.T. Oh, S.H. Kang, Y.A. Lim, et al., Epicatechin inhibits radiation-induced auditory cell death by suppression of reactive oxygen species generation, Neuroscience 199 (2011) 410–420, https://doi.org/10.1016/j.neuroscience.2011.09.012.
[47] J. Zhang, A. Xu, T. Niu, C. Liu, Y. Zhang, T. Li, et al., A unique radioprotective effect of resolvin E1 reduces irradiation-induced damage to the inner ear by inhibiting the inflammatory response, Radiat. Oncol. 15 (2020) 223, https://doi.org/10.1186/s13014-020-01662-9.
[48] X. Zhang, L. Hou, F. Li, W. Zhang, C. Wu, L. Xiang, et al., Piezo1-mediated mechanosensation in bone marrow macrophages promotes vascular niche regeneration after irradiation injury, Theranostics 12 (2022) 1621–1638, https://doi.org/10.7150/thno.64963.
[49] Y. Mizushima, C. Fujimoto, A. Kashio, K. Kondo, T. Yamasoba, Macrophage recruitment, but not interleukin 1 beta activation, enhances noise-induced hearing damage, Biochem. Biophys. Res. Commun. 493 (2017) 894–900, https://doi.org/10.1016/j.bbrc.2017.09.124.
[50] K. Xu, S. Chen, L. Xie, Y. Qiu, X.-Z. Liu, X. Bai, et al., The protective effects of systemic dexamethasone on sensory epithelial damage and hearing loss in targeted Cx26-null mice, Cell Death Dis. 13 (2022) 545, https://doi.org/10.1038/s41419-022-04987-3.
[51] B. Hu, C. Jin, H.-B. Li, J. Tong, X. Ouyang, N.M. Cetinbas, et al., The DNA-sensing AIM2 inflammasome controls radiation-induced cell death and tissue injury, Science (New York, N.Y.) 354 (2016) 765–768.
[52] S. Yamaga, A. Murao, G. Ma, M. Brenner, M. Aziz, P. Wang, Radiation upregulates macrophage TREM-1 expression to exacerbate injury in mice, Front. Immunol. 14 (2023) 1151250, https://doi.org/10.3389/fimmu.2023.1151250.

[53] M.J. Moravan, J.A. Olschowka, J.P. Williams, M.K. O'Banion, Brain radiation injury leads to a dose- and time-dependent recruitment of peripheral myeloid cells that depends on CCR2 signaling, J. Neuroinflammation 13 (2016) 30, https://doi.org/10.1186/s12974-016-0496-8.
[54] C. Blériot, S. Chakarov, F. Ginhoux, Determinants of resident tissue macrophage identity and function, Immunity 52 (2020) 957–970, https://doi.org/10.1016/j.immuni.2020.05.014.
[55] H. Kang, S.-C. Kim, Y. Oh, Fucoxanthin abrogates ionizing radiation-induced inflammatory responses by modulating sirtuin 1 in macrophages, Mar. Drugs 21 (2023), https://doi.org/10.3390/md21120635.
[56] Q. Wu, A. Allouch, I. Martins, N. Modjtahedi, E. Deutsch, J.L. Perfettini, Macrophage biology plays a central role during ionizing radiation-elicited tumor response, Biomed. J. 40 (2017) 200–211, https://doi.org/10.1016/j.bj.2017.06.003.
[57] C. Tabraue, P.C. Lara, M. De Mirecki-Garrido, J.V. De La Rosa, F. Lopez-Blanco, L. Fernandez-Perez, et al., LXR signaling regulates macrophage survival and inflammation in response to ionizing radiation, Int. J. Radiat. Oncol. Biol. Phys. 104 (2019) 913–923, https://doi.org/10.1016/j.ijrobp.2019.03.028.
[58] S. Rastogi, M. Boylan, E.G. Wright, P.J. Coates, Interactions of apoptotic cells with macrophages in radiation-induced bystander signaling, Radiat. Res. 179 (2013) 135–145, https://doi.org/10.1667/RR2969.1.
[59] Y. Chai, W. He, W. Yang, A.P. Hetrick, J.G. Gonzalez, L. Sargsyan, et al., Intratympanic lipopolysaccharide elevates systemic fluorescent gentamicin uptake in the cochlea, Laryngoscope 131 (2021) E2573–E2582, https://doi.org/10.1002/lary.29610.
[60] S.H. Bae, J.E. Yoo, Y.H. Choe, S.H. Kwak, J.Y. Choi, J. Jung, et al., Neutrophils infiltrate into the spiral ligament but not the stria vascularis in the cochlea during lipopolysaccharide-induced inflammation, Theranostics 11 (2021) 2522–2533, https://doi.org/10.7150/thno.49121.
[61] Y. Zhang, Y. Yang, Z. Xie, W. Zuo, H. Jiang, X. Zhao, et al., Decreased poly(ADP-ribose) polymerase 1 expression attenuates glucose oxidase-induced damage in rat cochlear marginal strial cells, Mol. Neurobiol. 53 (2016) 5971–5984, https://doi.org/10.1007/s12035-015-9469-7.
[62] G. Yiming, W. Fan, H. Wuhui, C. Ziyi, P. Jiaqi, Z. Yiqing, ROS-related disruptions to cochlear hair cell and stria vascularis consequently leading to radiation-induced sensorineural hearing loss, Antioxidants Redox Signal. (2023), https://doi.org/10.1089/ars.2022.0161.
[63] K. Hirose, S.-Z. Li, The role of monocytes and macrophages in the dynamic permeability of the blood-perilymph barrier, Hear. Res. 374 (2019) 49–57, https://doi.org/10.1016/j.heares.2019.01.006.
[64] M. Klein, U. Koedel, H.-W. Pfister, S. Kastenbauer, Morphological correlates of acute and permanent hearing loss during experimental pneumococcal meningitis, Brain Pathol. 13 (2003) 123–132.
[65] M.J. Polonenko, R.K. Maddox, Optimizing parameters for using the parallel auditory brainstem response to quickly estimate hearing thresholds, Ear Hear. 43 (2022) 646–658, https://doi.org/10.1097/AUD.0000000000001128.